Effects of Ultraviolet and Simvastatin Treatment on Titanium Implants Placed in Rabbit Tibia

Ji Hoon Jun

The Graduate School
Yonsei University
Department of Dentistry

Effects of Ultraviolet and Simvastatin Treatment on Titanium Implants Placed in Rabbit Tibia

A Dissertation
Submitted to the Department of Dentistry
and the Graduate School of Yonsei University
in partial fulfillment of the
requirements for the degree of
Doctor of Philosophy in Dental Science

Ji Hoon Jun

December 2021

This certifies that the dissertation
of Ji Hoon Jun is approved.

Thesis Supervisor: Hong Seok Moon

Jae-Hoon Lee

Kyung Chul Oh

Han-Sung Jung

Sung-Won Cho

The Graduate School
Yonsei University
December 2021

감사의 글

본 연구를 계획하고, 논문을 완성하기까지 세심한 지도와 아낌없는 지원, 진심 어린 격려로 저를 이끌어 주신 문홍석 지도교수님께 깊이 감사드립니다. 우여곡절이 많았던 동물 실험이었지만, 교수님의 지도로 잘 마무리할 수 있었습니다. 귀중한 시간을 내어 논문 심사를 맡아 저의 논문이 올바른 방향으로 작성될 수 있도록 소중한 조언을 해 주신 이재훈 · 오경철 · 정한성 · 조성원 교수님께 진심으로 감사드립니다.

또한, 치과의사로서 진실된 가치를 함양할 수 있도록 가르침을 주신 정문규 · 한동후 · 이근우 · 심준성 · 김선재 · 박영범 · 김지환 · 박지만 · 김종은 교수님께도 이 자리를 빌려 감사드립니다. 이 논문을 끝이 아닌 시작으로, 늘 겸손한 자세로 배우며 성장하는 치과의사가 되겠습니다.

연구 과정에 참여해 주셔서 실험이 원활히 진행될 수 있도록 도움을 주신 박규형 선생님, 정나래 선생님, Li Jiayi 에게도 감사를 드립니다. 또한 수련 과정부터 지금까지 힘들 때나 즐거울 때나 함께해 주고 연구를 도와준 연세대학교 치과대학병원 보철과 의국 동기 및 선후배들에게도 감사의 말을 전합니다. 특히, 같은 지도교수님 제자이자 군의관 선배로서 좋은 본보기가 되어 주신 전창주 선생님께 감사드립니다.

제가 이 자리에 올 수 있도록 사랑으로 키워 주신 아버지, 어머니께 감사드립니다. 마음이 따뜻하고 애정이 많은 여동생에게도 감사를 전합니다. 항상 저를 격려해주고 아껴 주시는 장인어른, 장모님께도 감사드립니다. 마지막으로 언제나 저의 곁에서 저를 응원해주고 제가 더 나은 사람이 될 수 있도록 헌신해주는 아내에게 고맙고 사랑한다는 말을 전합니다.

2021 년 12 월

전 지 훈

TABLE OF CONTENTS

LIST OF FIGURES ····· iii

LIST OF TABLES ····· iv

ABSTRACT ····· v

I. INTRODUCTION ····· 1

II. MATERIALS AND METHODS ····· 4

1. Materials ····· 4

1.1. Implant and Titanium Disc ····· 4

1.2. Xenogeneic Bone Graft Material ····· 4

1.3. Resorbable Barrier Membrane ····· 5

1.4. Simvastatin Solution ····· 5

2. UV Photofunctionalization ····· 5

3. Experimental Animals ····· 6

4. In Vivo Experimental Group Design and Sample Preparation ····· 6

5. Ethical Considerations ····· 9

6. Titanium Surface Characterization ····· 10

7. Surgical Procedure ····· 10

8. Animal Sacrifice and Sample Collection ····· 13

9. Histological Specimen Preparation ····· 14

10. Histomorphometric Analysis ····· 15

11. Statistical Analysis ····· 17

III. RESULTS ····· 18

1. FTIR Spectra of Titanium Discs ····· 18

2. Clinical Assessment of Experimental Animals ····· 20

3. Histological Examination and Quantitative Histomorphometry ····· 20

3.1. The 2-Week Group ····· 25

3.2. The 4-Week Group ····· 27

3.3. Comparison of the 2-Week and 4-Week Groups ····· 30

IV. DISCUSSION ····· 31

V. CONCLUSION ····· 39

REFERENCES ····· 40

ABSTRACT (KOREAN) ····· 52

LIST OF FIGURES

Figure 1. Flowchart of classification of the in vivo experimental groups ····· 8

Figure 2. Implantation sites of implants on the proximal tibial metaphysis in a rabbit ··· 9

Figure 3. Schematic diagram illustrating a cross-section of an implant placed in the rabbit tibia ····· 12

Figure 4. Clinical photograph illustrating implants placed in the rabbit tibia ····· 13

Figure 5. Measurement of bone-to-implant contact and bone area ····· 16

Figure 6. Fourier-transformed infrared spectra of the titanium discs ····· 19

Figure 7. Representative photomicrographs (12.5× magnification) of histological sections ····· 22

Figure 8. Representative photomicrographs (40× magnification) of histological sections ····· 23

Figure 9. Histomorphometric analyses of the 2-week experimental groups ····· 26

Figure 10. Histomorphometric analyses of the 4-week experimental groups ····· 28

Figure 11. Comparisons between the native sides and the grafted sides in the 4-week group, as evaluated by histomorphometry ····· 29

Figure 12. Comparisons between the 2- and the 4-week groups on the native sides, as assessed by histomorphometry ····· 30

LIST OF TABLES

Table 1. Descriptive statistics of BIC and BA values by groups and observation time ‥21

ABSTRACT

Effects of Ultraviolet and Simvastatin Treatment on Titanium Implants Placed in Rabbit Tibia

Ji Hoon Jun

Department of Dentistry

The Graduate School, Yonsei University

(Directed by Professor Hong Seok Moon, D.D.S., M.S.D., Ph.D.)

Effects of ultraviolet (UV) treatment and simvastatin (SIM) immersion on the osseointegration of sandblasted, large-grit, acid-etched (SLA) titanium dental implants were evaluated at two different time points in rabbit tibias, with or without xenogeneic bone graft material. Implants were categorized into four groups according to the surface treatment type. Twelve rabbits received two implants per tibia. A tibial defect model was created using a trephine bur, with implants in contact with the bone surface and bovine

bone graft materials for gap filling. The rabbits were sacrificed after 2 or 4 weeks. UV treatment or SIM immersion increased bone-to-implant contact (BIC) on native sides and BIC and bone area (BA) on grafted sides. The application of both treatments did not result in higher BIC or BA than a single treatment. It could be concluded that UV or SIM treatment of SLA titanium implants promotes osseointegration and new bone formation in tibias with or without xenogeneic bone graft material.

Keywords: Animal experiments; Bone implant interactions; Bone substitutes; Bone regeneration; Simvastatin; Ultraviolet; Titanium

Effects of Ultraviolet and Simvastatin Treatment on Titanium Implants Placed in Rabbit Tibia

Ji Hoon Jun

Department of Dentistry

The Graduate School, Yonsei University

(Directed by Professor Hong Seok Moon, D.D.S., M.S.D., Ph.D.)

I. INTRODUCTION

Immediate implant placement is the insertion of a dental implant directly into a fresh extraction socket site.[1] Its advantages include fewer surgeries, shorter total treatment time, less crestal bone loss, and favorable esthetic outcomes.[2] In the maxillary anterior region, immediate implants are usually placed in contact with the palatal bony wall to keep the labial wall intact and achieve favorable initial stability.[3] Consequently, in most cases, a gap defect is formed around the coronal area between the labial wall and the implant due to the discrepancy in size and shape between the implant and the socket.[4] Inserting xenogeneic

bone graft material such as bovine bone that provide structural support for new bone formation in conjunction with a resorbable membrane into these gaps has been proven to be an effective and predictable approach.[1,5-8]

Osseointegration is defined as direct contact at the microscopic level between living bone tissue and an implant without interposed soft tissue.[9-11] As osseointegration occurs, the percentage of bone-to-implant contact (BIC) increases, and stability of an implant also increases. With advances in implant dentistry, several methods for increasing BIC have been reported.

A recently discovered method to increase BIC is a physicochemical modification of implant surfaces using ultraviolet (UV) irradiation, in a process termed photofunctionalization. Many studies have demonstrated that this is a simple and effective method to enhance osseointegration.[12-15] UV pretreatment of titanium implants stimulates osseous healing by rendering the surface superhydrophilic and removing hydrocarbons adsorbed on the surface.[12-14,16-21] Furthermore, some studies have reported improved biological capabilities of UV treatment at the cellular and genetic levels.[12,18,22,23]

The application of biomaterials that can accelerate the bone healing process after implant placement has also drawn significant attention. One such example is statins.[24] Statins are cholesterol-lowering drugs that were originally developed to treat patients with cardiovascular disease. Interestingly, evidence has emerged showing that statins have beneficial effects on bone healing and turnover .[25,26] Statins act as dual agents that promote anabolic and inhibit catabolic functions in bone metabolism.[27] In vitro studies have shown

that statins induce osteoblast differentiation and enhance osteoblast viability.[28-30] Additionally, in vivo studies have proven that statins enhance the osseointegration of titanium implants.[27,31] Possible molecular mechanisms of statins related to bone remodeling reported in the literature are various and complex.[27,32-35] Simvastatin is the most frequently investigated statin and has been proven to be a potent agent for improving osseointegration.[34,36,37] However, most statins are degraded when administered orally due to the extensive first-pass effect in the liver, and less than 5% of the drug is available to the general circulation, with even lower amounts available to the bones.[37,38] Furthermore, statins have lower bone affinity.[34] Local statin delivery directly to the site of bone remodeling has been proposed to improve the bioavailability of statins to the bones.[24,39,40]

To date, no study has compared the effects of UV treatment and simvastatin immersion or investigated the synergistic effect of the two methods in osseous healing around implants over time. Furthermore, there is no report on how the application of UV and simvastatin on implant surfaces affects BIC and new bone formation in peri-implant defects filled with bone graft material. Therefore, considering the necessity for reinforcing the bone repair around implants, the author sought to investigate the effect of irradiating the implants with UV or immersing it in a simvastatin solution on implants placed in peri-implant circumferential gap defects prepared in an animal model, mimicking immediate implant placement. The null hypothesis was that there would be no difference in BIC and new bone formation between the control and UV- and/or simvastatin-treated groups with or without bone grafting.

II. MATERIALS AND METHODS

1. Materials

1.1. Implant and Titanium Disc

Forty-eight SLA surface-treated internal conical-type titanium dental implants (Dentium NR line; Dentium, Suwon, South Korea), measuring 3.1 mm in diameter and 7 mm in length, and two titanium discs with SLA surface, 10 mm in diameter and 2 mm in thickness, prepared from pure grade IV titanium (Dentium) were utilized in the study. A short, narrow diameter implant was selected considering the average width and thickness of the rabbit tibia, with reference to previous studies.[1,17,41-45] In brief, SLA surface treatments were performed by sandblasting with aluminum oxide and acid etching with hydrochloric acid. The implants were manufactured at the same time and kept in separate sealed containers.

1.2. Xenogeneic Bone Graft Material

Bio-Oss (Geistlich Pharma AG, Wolhusen, Switzerland) was used as the xenogeneic bone graft material. Its particle size ranged from 250 to 1000 μm in diameter. This material is sterilized bovine bone with all organic components removed.

1.3. Resorbable Barrier Membrane

GENOSS collagen membrane (Genoss, Suwon, South Korea) was used as a barrier membrane. It is a sterilized and biodegradable membrane made from bovine tendon (type I collagen). The collagen component of the membrane is chemically crosslinked, delaying the collapse of the barrier and permitting sufficient time for osseous maturation with biocompatibility.[46]

1.4. Simvastatin Solution

Solid simvastatin (Sigma-Aldrich, St. Louis, MO, USA) was reconstituted in a dimethyl sulfoxide solvent (Sigma-Aldrich) to a concentration of 25 mM, and the solution was diluted to 0.5 mM in phosphate-buffered saline (PBS; GIBCO, Thermo Fisher Scientific Inc., Waltham, MA, USA). The solution was sterilized by filtration through a 0.22 μm polyvinylidene difluoride membrane (Sartorius, Göttingen, Germany) under sterile conditions and diluted to working concentrations using PBS.

2. UV Photofunctionalization

UV photofunctionalization was performed by irradiating samples with UV light for 15 min using a specialized instrument (TheraBeam SuperOsseo; Ushio Inc., Tokyo, Japan) using an exposure time based on earlier studies.[16,47] Specifications of the device were as follows: input voltage of AC 100 to 240 V ± 10%, input current of 2.2 A in maximum, temperature of 15–30 °C, humidity of 20–70%, and altitude below 2000 m.

Multiple UV lamps were utilized to create the UV light as a mixed spectrum at wavelengths of 360 nm (0.05 mW/cm^2) and 250 nm (2 mW/cm^2).[48] Inside the device, the lamps were arranged to irradiate a sample in all directions homogeneously.

3. Experimental Animals

Twelve specific pathogen-free female New Zealand White rabbits (3-month-old and weighing 3 ± 0.5 kg), without any genetic modifications or systemic diseases, were enrolled in this animal trial. Each rabbit was housed in an individual cage and kept under standard laboratory conditions at 24 °C ambient temperature in a 12 h dark/light cycle. The location of the cage was randomly assigned. Standard diet and water were provided ad libitum.

4. In Vivo Experimental Group Design and Sample Preparation

Forty-eight SLA implants were divided equally into control and three test groups according to the treatment methods used, as follows (Figure 1):

- Group C: implants placed without any treatment in rabbits sacrificed at 2 weeks (Group C-2) or 4 weeks (Group C-4)

- Group U: implants irradiated with UV immediately before implantation, but not coated with simvastatin, in rabbits sacrificed at 2 weeks (Group U-2) or 4 weeks (Group U-4)

- Group S: implants immersed in simvastatin solution for 24 h in separate sealed containers without UV exposure in rabbits sacrificed at 2 weeks (Group S-2) or 4 weeks (Group S-4)
- Group SU: implants first immersed in simvastatin solution for 24 h and then irradiated with UV immediately before surgery in rabbits sacrificed at 2 weeks (Group SU-2) or 4 weeks (Group SU-4)

Each rabbit received two implants per tibia, i.e., four implants per rabbit. Group C and group U implants were placed in the left tibia, and group S and group SU implants were placed in the right tibia (Figure 2). The implants were placed symmetrically to minimize differences in the surgical sites. The 12 rabbits were separated into two groups to observe differences according to the healing time. Six rabbits were allowed a healing period of 2 weeks postoperatively (2-week group) and the other six a healing period of 4 weeks (4-week group). The required sample size was calculated with reference to related studies.[49,50]

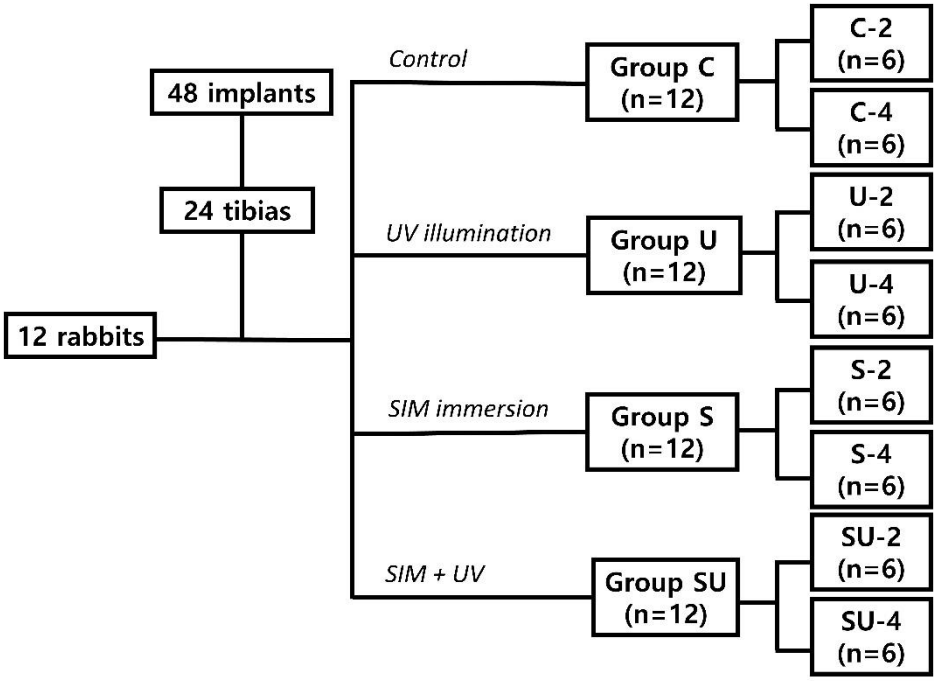

Figure 1. Flowchart of classification of the in vivo experimental groups. Group C, control group: implants without additional surface treatments in rabbits sacrificed at 2 weeks (C-2) or 4 weeks (C-4). Group U: implants irradiated with UV without immersion in SIM solution in rabbits sacrificed at 2 weeks (U-2) or 4 weeks (U-4). Group S: implants immersed in SIM solution for 24 h without UV exposure in rabbits sacrificed at 2 weeks (S-2) or 4 weeks (S-4). Group SU: implants first immersed in SIM solution for 24 h followed by UV irradiation before placement in rabbits sacrificed at 2 weeks (SU-2) or 4 weeks (SU-4). UV, ultraviolet; SIM, simvastatin.

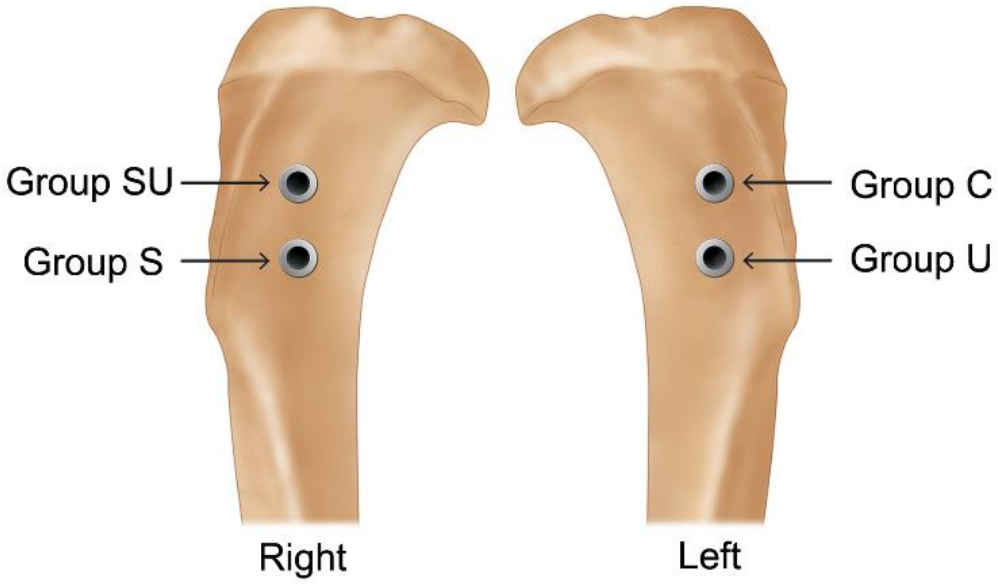

Figure 2. Implantation sites of implants on the proximal tibial metaphysis in a rabbit.

5. Ethical Considerations

All procedures, including animal selection, care, preparation, general anesthesia, and surgical steps, were approved by the Institutional Animal Care and Use Committee (Yonsei Medical Center, Seoul, Korea; Approval No. 2019-0157). The housing protocol suggested by the Association for Assessment and Accreditation of Laboratory Animal Care International guidelines was followed. In addition, the study design complied with the ARRIVE guidelines.

6. Titanium Surface Characterization

The SLA surface-treated titanium disc and the same kind of disc, but further immersed in simvastatin solution for 24 h, were analyzed by attenuated total reflection Fourier-transform infrared (ATR-FTIR) spectrometer (Vertex 70; Bruker, Ettlingen, Germany) to characterize the functional groups present on the surfaces. Each disc was fixed on a single reflection horizontal ATR accessory to perform analysis. FTIR spectra were measured in the wavenumber range of 4000–400 cm^{-1} at the transmittance mode, cumulating 20 scans at a resolution of 4 cm^{-1}.

7. Surgical Procedure

The in vivo experiment was conducted at the Avison Biomedical Research Center. One blinded researcher, unaware of the time of sacrifice and the group to which an implant belonged, placed the implants, and performed bone grafts. Two blinded researchers assisted the surgical procedure. One researcher, aware of the group allocation of the implants, prepared implants in a separate room and offered them to the blinded researcher.

After an acclimation period of 1 week, the surgical procedure was implemented as described previously.[1,17,41,42,44] General anesthesia was administered by inhalation of 2–2.5% isoflurane (Ifran; Hana Pharm Co. Ltd., Seoul, South Korea), an intramuscular injection of tiletamine/zolazepam (10 mg/kg, Zoletil-50; Virbac, Carros, France), and an intravenous injection of xylazine (2.3 mg/kg, Rompun; Bayer Korea, Seoul, South Korea). The surgical site was shaved and disinfected with povidone-iodine solution. Local anesthesia was

performed in the surgical area through an injection of 2% lidocaine with 1:80,000 epinephrine (2% Lidocaine hydrochloride injection; Huons Co., Ltd., Seongnam, Korea).

After skin preparation and sterile draping, a 5.0 cm linear, longitudinal incision was made under aseptic conditions on the medial side of the tibia, immediately below the knee, and a full-thickness flap was raised to expose the underlying tibial bone. Two surgical circumferential defects of 5 mm in diameter and 4 mm in depth were created in the proximal surface of both the left and right tibial metaphysis, using a 5 mm diameter trephine bur (Dentium), separated by 5 mm. Additional osteotomy was performed on the prepared bone bed using a 2.0 mm pilot drill and a 3.1 mm guide drill. A 0.9% chilled saline solution was continuously sprayed over the drill site to avoid overheating. During the osteotomy procedure, sequential drilling was performed through the opposite side of the tibia to achieve bicortical fixation of the implants. The implants were placed in contact with one side of the circular defects under 30 N·cm of torque using an electric motor with a contra-angle handpiece. The implants were engaged bicortically, and cover screws were screwed over them.

After implant placement, bovine bone material was inserted to fill the peri-implant defects (Figures 3 and 4). A trimmed GENOSS collagen membrane was applied to cover the defect fully. The fascia and cutaneous tissue were repositioned and sutured without tension using 4-0 synthetic resorbable materials (Vicryl; Ethicon, Somerville, NJ, USA), and the skin was sutured with monofilament nylon (4-0 Monosyn; Johnson & Johnson International, Edinburgh, Scotland). A general analgesic (0.1 mg/kg/day, Meloxicam;

Metacam, Boehringer Ingelheim, Ingelheim, Germany) and an antibiotic (10 mg/kg/day, Enrofloxacin; Baytril, Bayer, Seoul, South Korea) were administered intravenously for 5 days postoperatively.

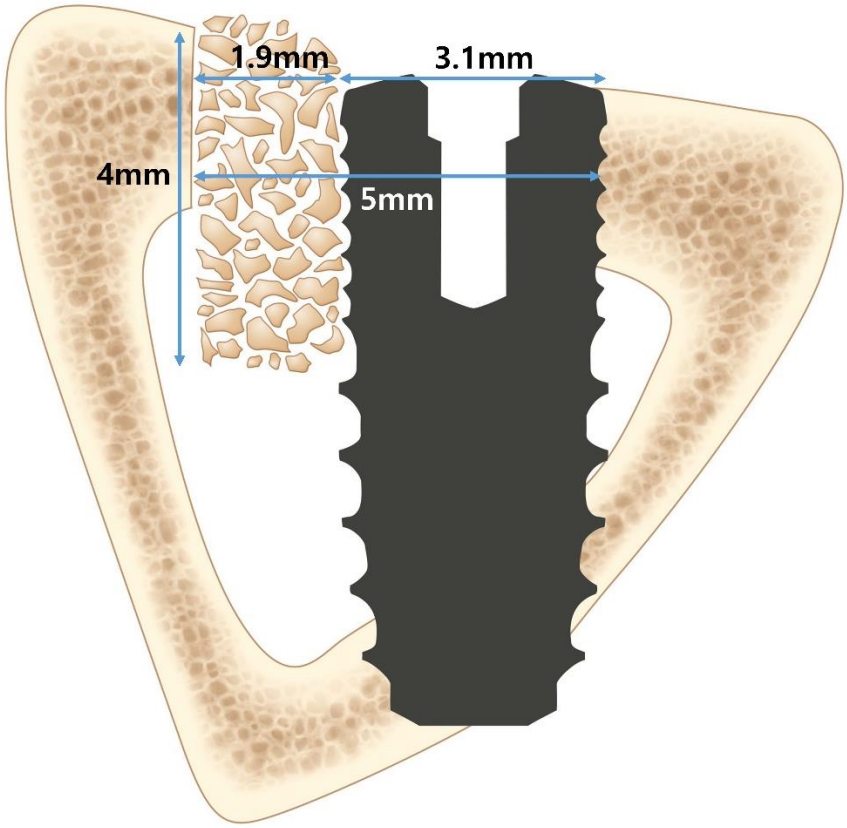

Figure 3. Schematic diagram illustrating a cross-section of an implant placed in the rabbit tibia. Particles contacting the implant represent bovine bone graft material.

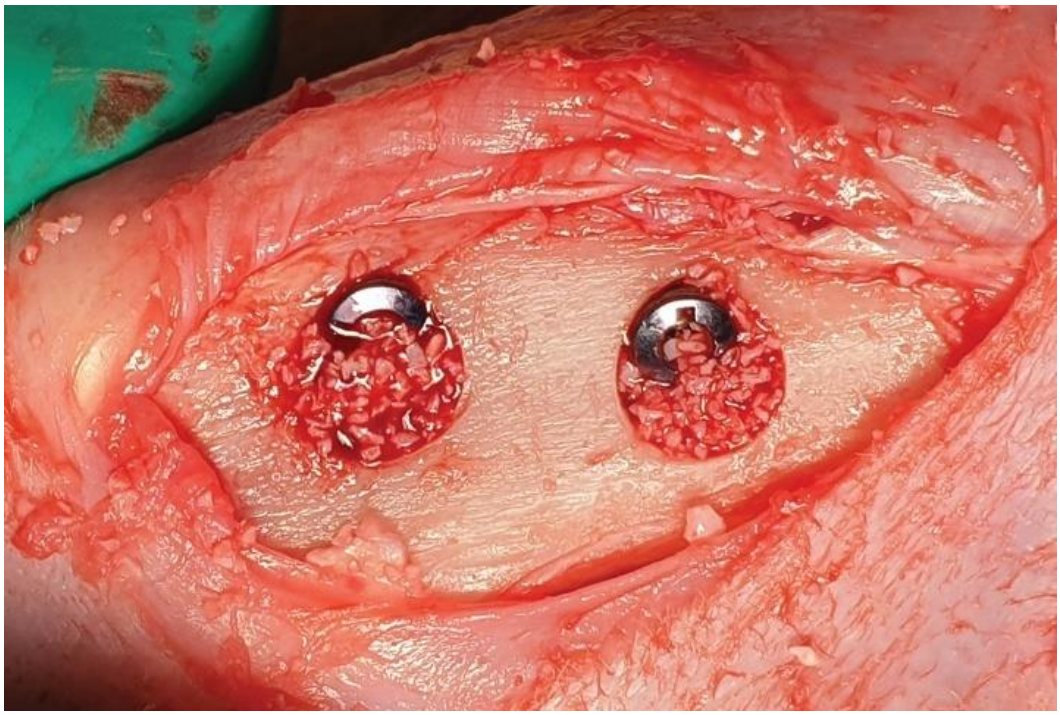

Figure 4. Clinical photograph illustrating implants placed in the rabbit tibia. Xenogeneic graft material is placed in the gap defects.

8. Animal Sacrifice and Sample Collection

The rabbits were sacrificed at either 2 or 4 weeks postoperatively (6 rabbits at each time point). General anesthesia was induced by subcutaneous injection of 5 mg/kg alfaxalone (Alfaxan; Careside, Seongnam, South Korea) and 0.25 mg/kg medetomidine (Tomidin; Provet Veterinary Products, Istanbul, Turkey), intramuscular injection of 2.3 mg/kg xylazine, followed by intravenous injection of 0.5 mg/kg alfaxalone and 0.12 mg/kg medetomidine. To induce euthanasia, 50 mg tramadol (Trodon injection; Ajupharm, Seoul,

South Korea) and 0.3 g potassium chloride (Potassium chloride-40 injection; Dai Han Pharm, Seoul, South Korea) were intravenously injected. The tibias were surgically reopened, and the implants and the block of bone surrounding the tibia head were harvested en bloc. The exclusion criteria for the sample were the presence of complications such as tibial fracture, infection, or inflammation.

9. Histological Specimen Preparation

The samples were stored in a fixation solution for 2 weeks (10% Formaldehyde solution buffered with 0.1 M phosphate solution, pH 7.2; Sigma-Aldrich). Subsequently, they were washed in running water and dehydrated in a series of increasing ethanol concentrations, in the order of 70%, 80%, 90%, and 100%. Thereafter, the dehydrated specimens, without being decalcified, were embedded in a methyl methacrylate-based resin (Technovit 7200 VLC; Kulzer & Co, Norderstedt, Germany), cured under a UV instrument (Kulzer Exact 520; Kulzer & Co, Norderstedt, Germany). Non-decalcified ground sections of the implants and surrounding bone tissue were fabricated following the method suggested by Donath and Breuner[51]. The specimens were sectioned in the longitudinal plane through the middle of the implants and reduced to a thickness of 15 μm using a micro-grinding machine (Kulzer Exact 400CS; Kulzer & Co, Norderstedt, Germany). Hematoxylin and eosin staining was performed on the entirety of the slices.

10. Histomorphometric Analysis

After microscopic observation, histological images were captured at 12.5× and 40× magnification using a digital camera (Polaroid DMC2 digital microscope camera; Polaroid Corporation, Cambridge, MA, USA) attached to a light microscope (Olympus BX50; Olympus Optical, Tokyo, Japan). Quantification was performed under 40× magnification with image analysis software (ImageJ; NIH, Bethesda, MD, USA; http://imagej.nih.gov/ij/index.html). As in previous studies, an area within the three best consecutive threads engaged in the upper cortical bone region was defined as the region-of-interest (ROI).[52-54] The measurement followed the method suggested by Lee et al.[18] (Figure 4). Within the ROI, the following primary outcome measures were evaluated by two blinded and trained examiners, and the average values were used for statistical analysis. BIC (%) was calculated as “bone contact length within threads/overall length of threads”. Bone area (BA, %) was calculated as “area of newly formed bone between threads/overall area between threads”.

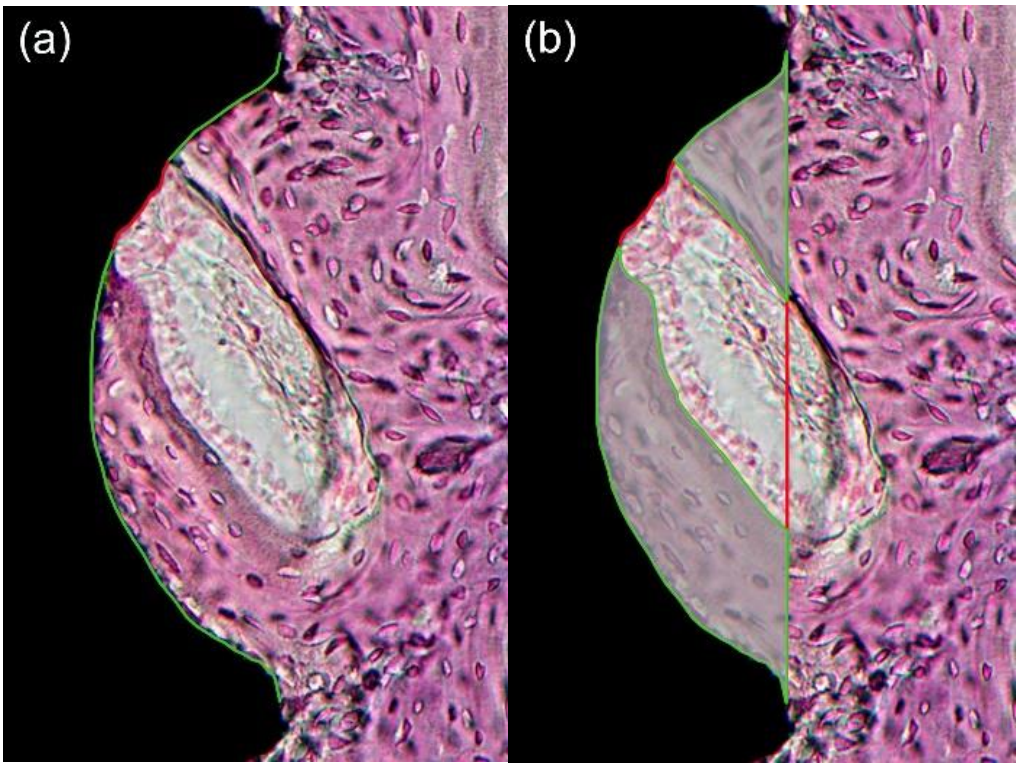

Figure 5. Measurement of bone-to-implant contact and bone area. **(a)** Bone-to-implant contact calculated by the length of the green lines divided by the total length of the well (green and red lines); **(b)** Bone area calculated by the area marked with green lines divided by the total area of the well. Note that the region-of-interest (ROI) was defined as an area within the three best consecutive threads engaged in the upper cortical bone, and therefore, a total of three threads were used for the calculation. Only one third of ROI is shown for simplicity.

11. Statistical Analysis

Statistical analysis was performed using SPSS version 25 (IBM Corp., Armonk, NY, USA). Normality of all the data were evaluated using the Shapiro–Wilk test. The data were not normally distributed; thus, the Kruskal–Wallis test was used to determine whether the median values of BIC and BA differed significantly among groups at each time point. This was followed by the Mann–Whitney U test with Bonferroni correction (0.05/3=0.017) for multiple comparisons. Next, a two-way analysis of variance followed by post hoc Tukey's test was used to determine whether the median values of BIC and BA differed significantly between the 2- and 4-week time points in each group. Subsequently, the Mann–Whitney U test was used for multiple comparisons. The level of statistical significance was set at $\alpha = 0.05$. GraphPad Prism 7.0 software (GraphPad Software Inc., La Jolla, CA, USA) was used to visualize the data.

III. Results

1. FTIR Spectra of Titanium Discs

Figure 5 shows the FTIR spectra of the titanium discs. The spectrum of the disc immersed in simvastatin solution resembled that of simvastatin reported in the literature.[55,56] The prominent bands of the OH stretching vibrations (3600–3200 cm^{-1}) and the carbonyl C=O stretching vibration (1800–1600 cm^{-1}) were observed. The fingerprint region occurring at < 1500 cm^{-1} indicated the presence of simvastatin adsorbed onto the titanium surface. The spectral analysis confirmed the alteration of the surface of the titanium disc upon simvastatin treatment from a chemical perspective.

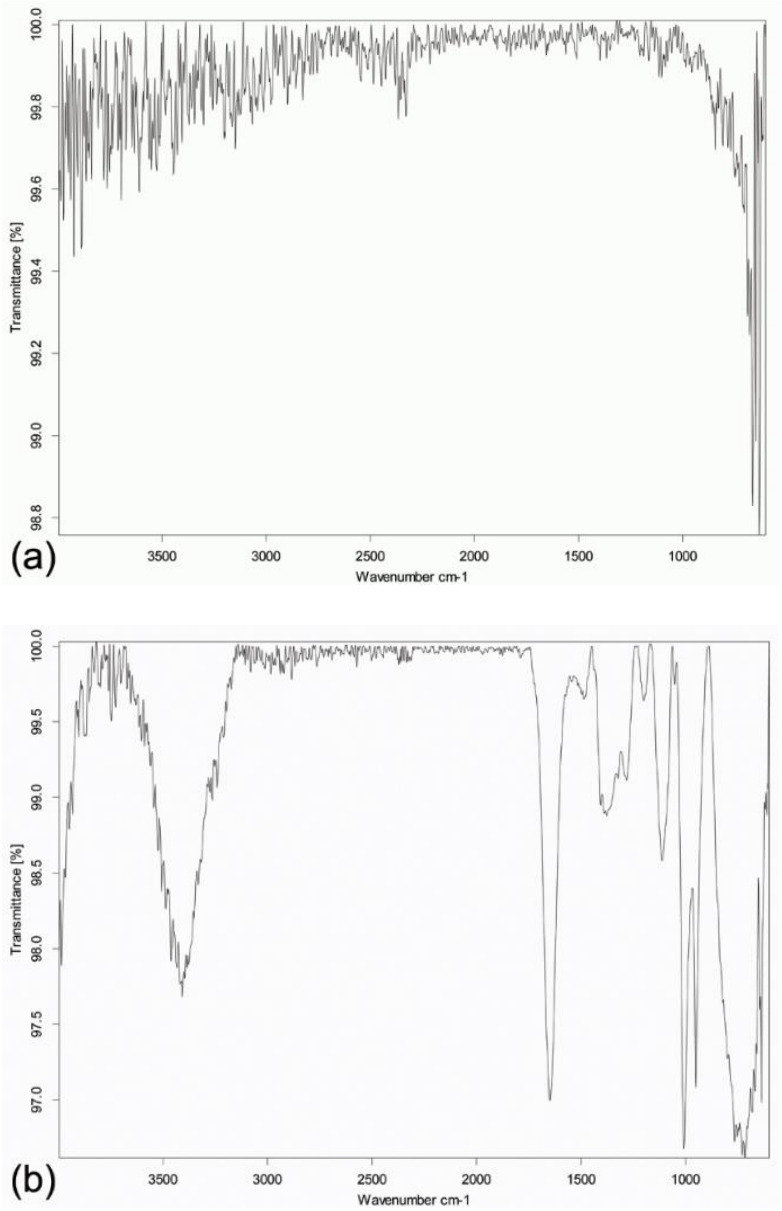

Figure 6. Fourier-transformed infrared spectra of the titanium discs. **(a)** Spectrum of the sandblasted, large-grit, acid-etched surface-treated titanium disc. **(b)** Spectrum of the same kind of disc but further immersed in simvastatin solution.

2. Clinical Assessment of Experimental Animals

During the postsurgical period, all rabbits recovered uneventfully. No signs of the complications stated in the exclusion criteria were observed. After sacrifice, a normal periosteum was found in all specimens, and no clinical signs of adverse tissue reactions were observed at a macroscopic level. All implants were still in situ and available for histological analysis; therefore, all samples were included in subsequent analyses.

3. Histological Examination and Quantitative Histomorphometry

As both the native and grafted sides of each implant were examined, 96 sites were analyzed in total. The mean value of the interclass correlation coefficient was larger than 0.8, implying a strong level of agreement between the examiners. The average values of the measurements made by the two examiners were used.

Representative photomicrographs are shown in Figures 7 and 8; the results of the histomorphometric analyses are summarized Table 1 and are illustrated in Figures 9–11. Apical migration of the epithelium and connective tissue was not observed in any of the samples. In the 2-week group, on the grafted sides, a sparse amount of new bone in the vicinity of the implants was observed in the majority of the specimens, regardless of the method of surface modification used (Figure 8b, d). Therefore, the examiners were unable to perform histomorphometric measurements.

Table 1. Descriptive statistics of BIC and BA values by groups and observation time

Time/Group	BIC (%)				BA (%)			
2 weeks (native)	Mean ± SD	Min	Med	Max	Mean ± SD	Min	Med	Max
C-2	59.3 ± 3.2	53.5	60.5	62.3	66.9 ± 8.9	59.1	62.8	78.9
U-2	85.2 ± 6.7	74.8	84.5	93.7	68.3 ± 10.9	52.6	72.7	79.3
S-2	80.9 ± 3.9	75.5	80.1	86.3	73.5 ± 5.7	63.0	75.5	77.8
SU-2	83.2 ± 6.1	76.4	83.7	89.5	75.6 ± 10.3	57.2	77.9	84.2
4 weeks (native)	Mean ± SD	Min	Med	Max	Mean ± SD	Min	Med	Max
C-4	66.2 ± 5.7	57.4	66.4	74.5	80.7 ± 8.2	69.0	81.2	90.4
U-4	91.2 ± 4.0	85.1	90.6	96.3	91.9 ± 4.2	84.0	93.2	95.6
S-4	85.2 ± 4.7	78.6	86.0	91.8	87.0 ± 8.7	72.8	89.7	95.2
SU-4	84.6 ± 5.7	76.9	83.8	92.0	87.1 ± 6.9	76.2	88.7	96.5
4 weeks (grafted)	Mean ± SD	Min	Med	Max	Mean ± SD	Min	Med	Max
C-4	67.0 ± 7.3	59.1	66.5	78.0	67.0 ± 10.0	57.6	64.4	79.0
U-4	89.5 ± 6.4	79.1	90.0	96.7	91.4 ± 10.0	73.7	95.9	100.0
S-4	86.7 ± 7.0	78.6	84.5	98.0	86.1 ± 5.8	79.9	85.8	94.6
SU-4	90.5 ± 4.9	85.6	89.3	100.0	89.0 ± 4.9	84.0	87.9	94.9

Abbreviations: BIC, bone-to-implant contact; BA, bone area; SD, standard deviation; Min, minimum; Med, median; Max, maximum.

Data are expressed as mean ± standard deviations.

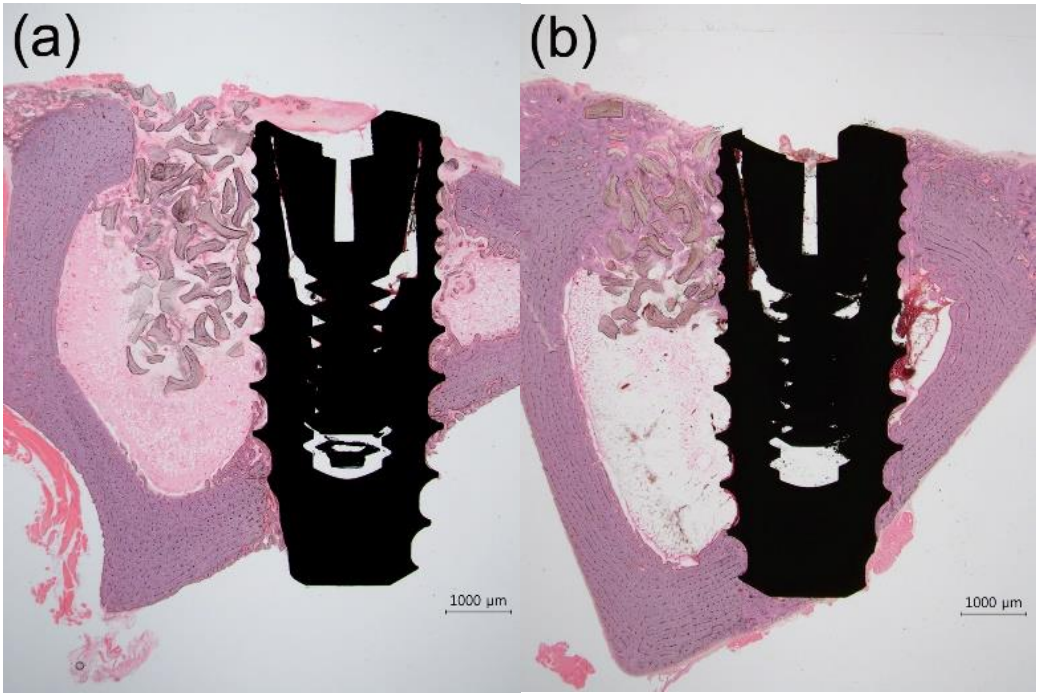

Figure 7. Representative photomicrographs (12.5× magnification) of histological sections. Hematoxylin and eosin-stained histological sections of rabbit tibias at the implanted regions are shown. **(a)** 2-week group; **(b)** 4-week group. Scale bars: 1000 μm.

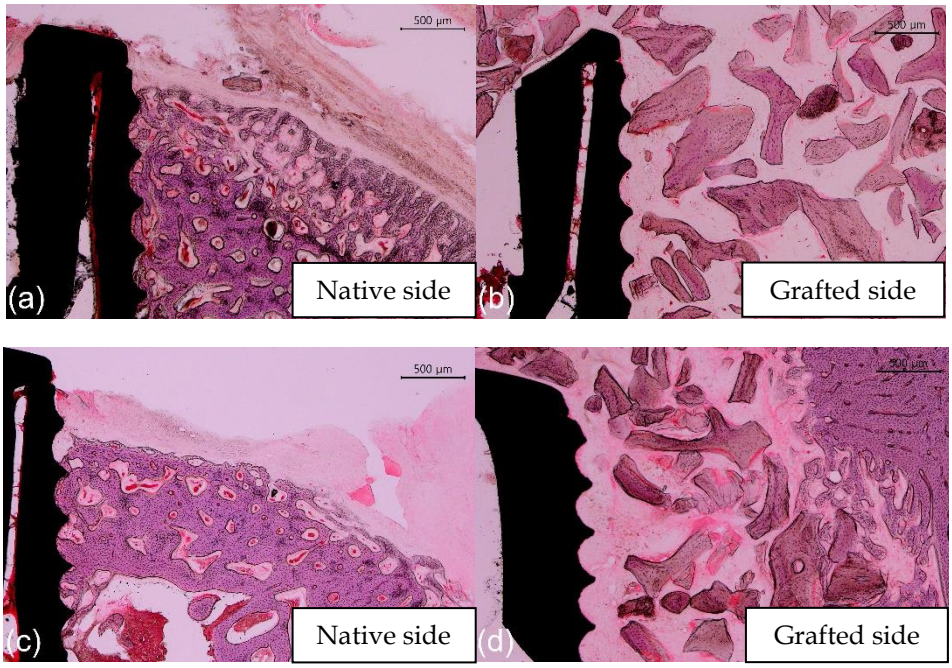

Figure 8. Representative photomicrographs (40× magnification) of histological sections. Hematoxylin and eosin-stained histological sections of rabbit tibias at the implanted regions are shown. **(a)** Group C-2, native side; **(b)** Group C-2, grafted side; **(c)** Group SU-2, native side; **(d)** Group SU-2, grafted side; (continued the next page)

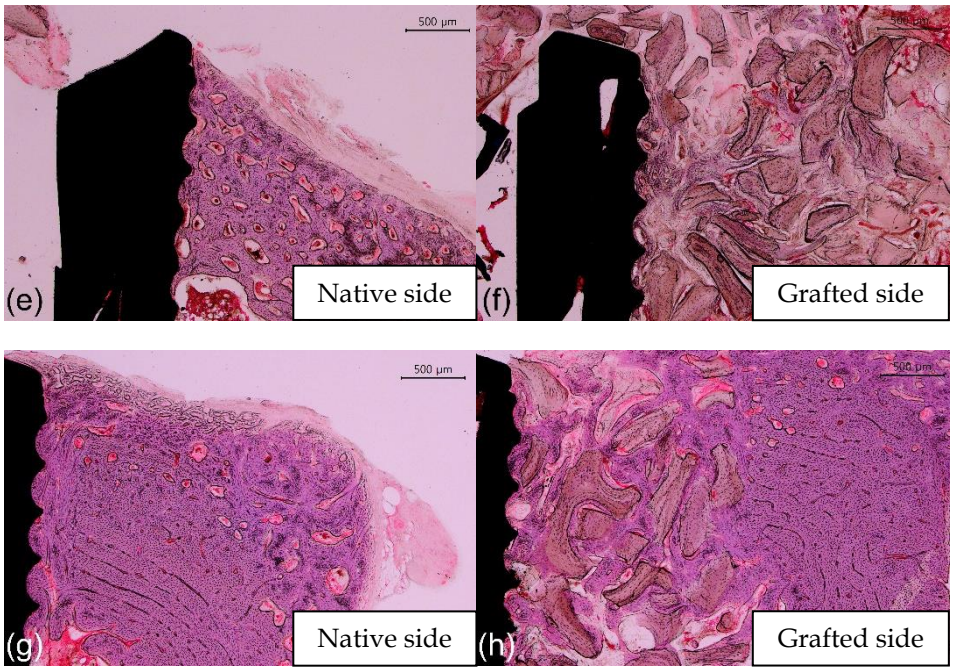

Figure 8 (continued). (e) Group C-4, native side; **(f)** Group C-4, grafted side; **(g)** Group SU-4, native side; and **(h)** Group SU-4, grafted side. Note the sparse amount of new bone on the grafted side in 2-week groups. Scale bars: 500 μm.

3.1. The 2-Week Group

In the native sides, bone neoformation was found at the bone/implant interface in cortical bone (Figure 8a, c). The mean BIC values of group U-2, S-2, and SU-2 were 85.2%, 80.9%, and 83.2% respectively. These values were significantly higher (approximately 20%) than the BIC value (59.3%) of group C-2 ($p < 0.05$) (Figure 9a). There was no statistically significant difference in the BIC values among the experimental groups ($p > 0.05$). The BA values did not differ significantly among the four groups ($p > 0.05$) (Figure 9b).

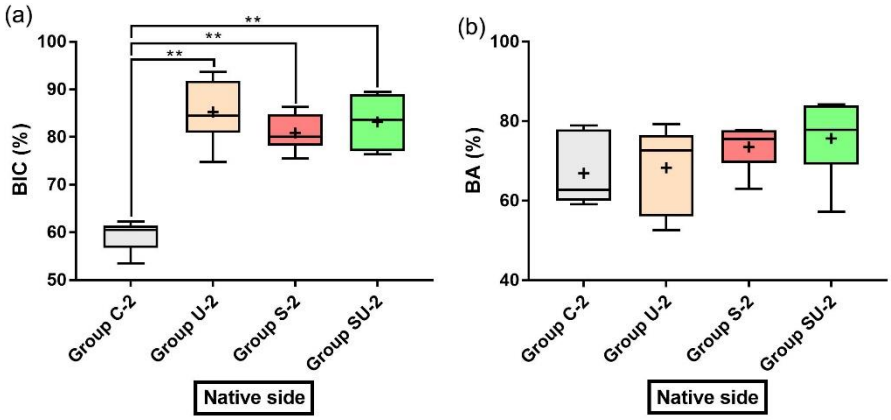

Figure 9. Histomorphometric analyses of the 2-week experimental groups. The grafted sides of 2-week groups were not analyzed due to a sparse amount of new bone in the vicinity of the implants. **(a)** BIC at the native side of the 2-week group; **(b)** BA at the native side of the 2-week group. Asterisks indicate statistically significant differences among the groups (** $p < 0.01$). The lines inside the boxes indicate median values, and the cross signs inside the boxes indicate mean values. The borders of the boxes indicate the 25th and 75th percentiles. The whiskers indicate the minimum and maximum values. BIC, bone-to-implant contact; BA, bone area.

3.2. The 4-Week Group

In the sides contacting the innate bone, the amount of newly formed bone in direct contact with the implant surface was more prominent in comparison with that in the 2-week group (Figure 8e, g). The mean BIC values of group U-4, S-4, and SU-4 were 91.2%, 85.2%, and 84.6%, respectively. Similar to the 2-week group, the BIC values of group U-4, S-4, and SU-4 were approximately 20% higher than the BIC value (66.2%) of group C-4 ($p < 0.05$) (Figure 10a). There was no statistically significant difference in the BIC values among the experimental groups ($p > 0.05$). The BA values did not differ significantly among the four groups ($p > 0.05$) (Figure 10b). The overall numerical tendency was analogous to that of the 2-week group.

On the grafted sides, newly formed bone was observed at the bone/implant interface and around the biomaterial (Figure 8f, h). The bone graft material was not degraded during this period and was discernible from the newly formed bone. Both the BIC and BA values of group U-4, S-4, and SU-4 were significantly higher (about 20%) than those of group C-4 ($p < 0.05$) (Figure 10c, d). There was no significant difference in either parameter among group U-4, S-4, and SU-4 ($p > 0.05$). When the native and grafted sides in the 4-week group were compared, there was no significant difference between them in terms of BIC and BA ($p > 0.05$), regardless of the surface treatment methods used (Figure 11).

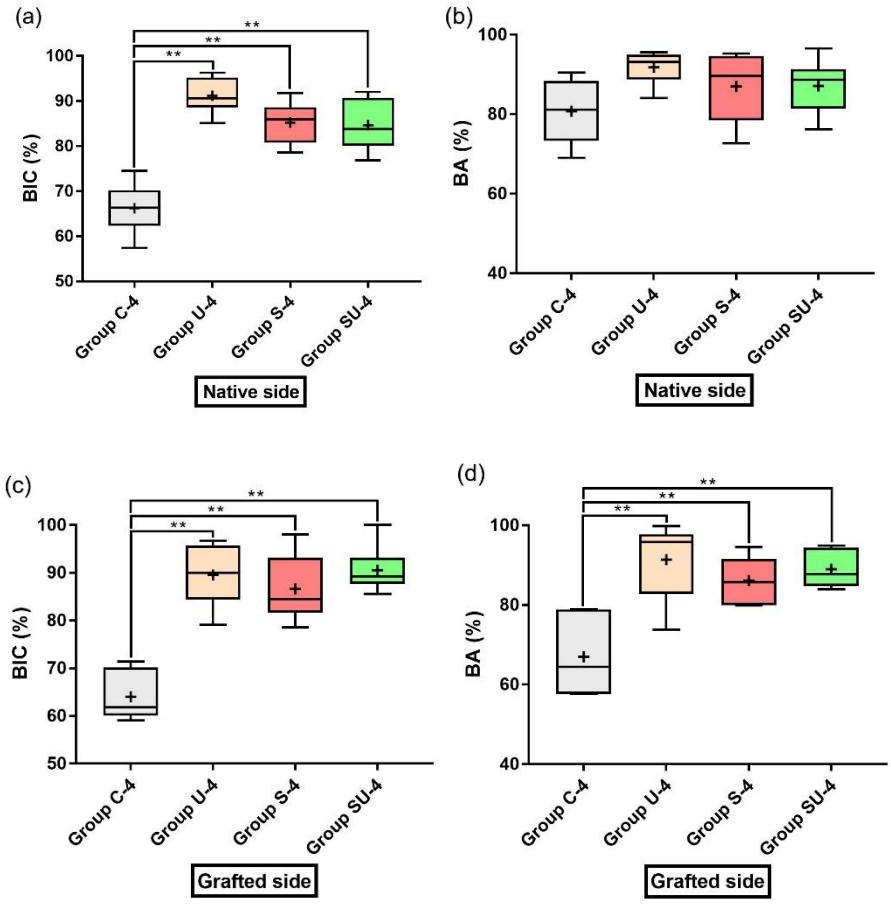

Figure 10. Histomorphometric analyses of the 4-week experimental groups. **(a)** BIC at the native side of the 4-week group; **(b)** BA at the native side of the 4-week group; **(c)** BIC at the grafted side of the 4-week group; and **(d)** BA at the grafted side of the 4-week group. Asterisks indicate statistically significant differences among the groups (** $p < 0.01$). The lines inside the boxes indicate median values, and the cross signs inside the boxes indicate mean values. The borders of the boxes indicate the 25th and 75th percentiles. The whiskers indicate the minimum and maximum values. BIC, bone-to-implant contact; BA, bone area.

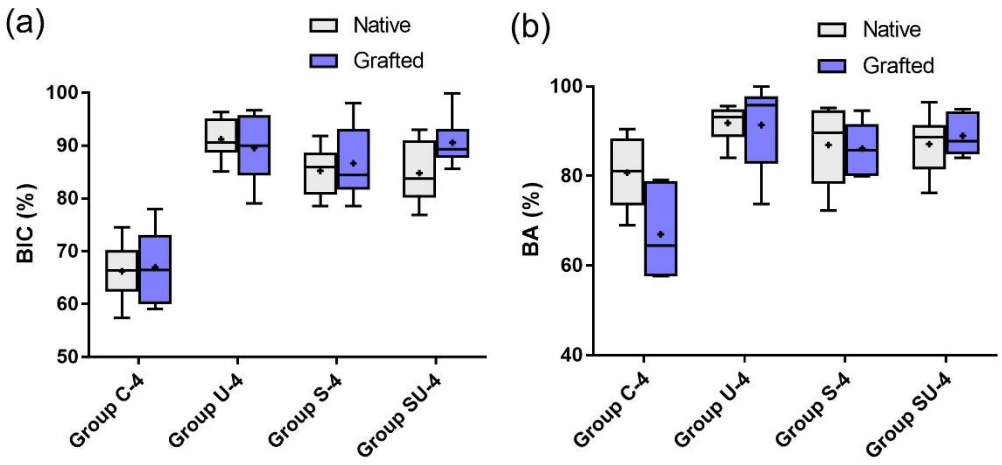

Figure 11. Comparisons between the native sides and the grafted sides in the 4-week group, as evaluated by histomorphometry. **(a)** BIC; **(b)** BA. Data are expressed as mean ± standard deviations. Error bars show the standard deviations. The lines inside the boxes indicate median values, and the cross signs inside the boxes indicate mean values. The borders of the boxes indicate the 25th and 75th percentiles. The whiskers indicate the minimum and maximum values. BIC, bone-to-implant contact; BA, bone area.

3.3. Comparison of the 2-Week and 4-Week Groups

In the native sides, group C exhibited a significant increase in both BIC (about 10% higher) and BA (about 20% higher) ($p < 0.05$) (Figure 12). In contrast, the group U, S, and SU displayed a significant increase in BA (about 20% higher) only ($p < 0.05$).

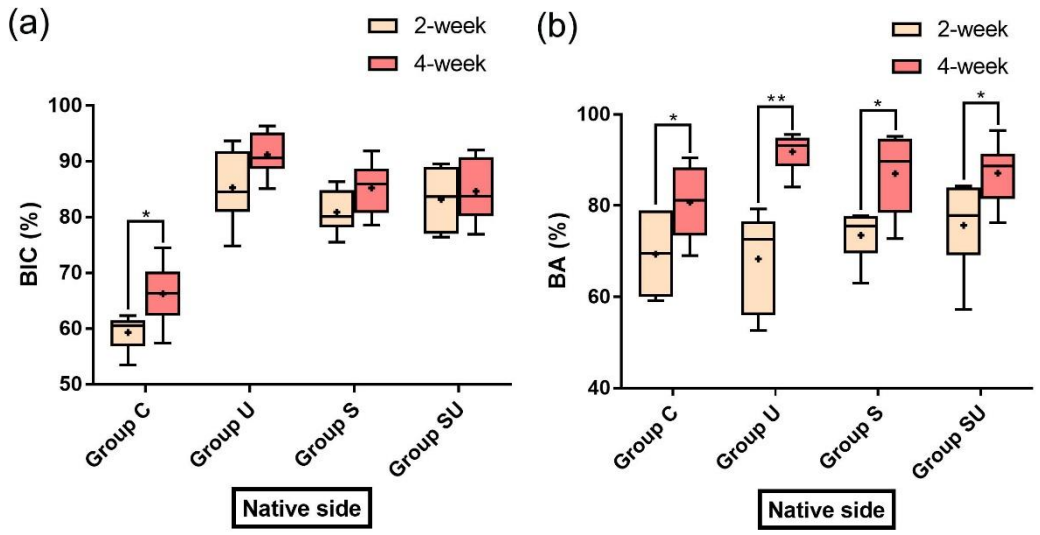

Figure 12. Comparisons between the 2- and the 4-week groups on the native sides, as assessed by histomorphometry. **(a)** BIC; **(b)** BA. Data are expressed as mean ± standard deviations. Asterisks indicate statistically significant differences among the groups (* $p < 0.05$ and ** $p < 0.01$). The lines inside the boxes indicate median values, and the cross signs inside the boxes indicate mean values. The borders of the boxes indicate the 25th and 75th percentiles. The whiskers indicate the minimum and maximum values. BIC, bone-to-implant contact; BA, bone area.

IV. Discussion

The null hypothesis of the present study was rejected because UV treatment and/or simvastatin immersion of implants resulted in considerable bone formation in vivo at the bone-implant interface, both in surfaces contacting the pristine bone and in the neighboring gap defects filled with xenogeneic bone substitutes. To the best of the author's knowledge, no previous study has integrated UV-treated and simvastatin-saturated implants along with bone-grafting procedures in peri-implant defects or compared the effects of UV, simvastatin, and the combination of both.

Healing periods of 2 and 4 weeks were adopted based on previous studies.[17,41,57] To measure the efficacy of UV and/or simvastatin to facilitate osseointegration, the time window was set earlier than the time required for a titanium implant to be osseointegrated in a rabbit long bone under normal conditions.[58,59] The results showed that, in the native sides, a higher degree of osseointegration in the experimental groups (group U, S, and SU) was observed at 2 and 4 weeks postimplantation in rabbits, as demonstrated by the BIC values. Therefore, modification of the implant surface by UV pretreatment or simvastatin immersion seems to promote osseointegration.

In the 2-week group, on the grafted sides, a scarce amount of new immature bone was formed between the implant threads to perform histometric analysis, implying that 2 weeks of healing was not long enough. This is in agreement with a study by Araújo et al.[60], in which a delay in bone repair was reported for extraction sockets filled with bone

substitutes. On the grafted side, the implant surface is distant from the osteogenic sources - that is, the pristine bone - which results in a relative lack of new bone formation during such a short period. Perhaps setting healing period to 3 weeks, instead of 2 weeks, would have been better to observe newly formed bone on the grafted sides and to appreciate differences between the control group and the experimental groups. Nevertheless, in the 4-week group, both BIC and BA could be measured, and the experimental groups presented higher values. This shows that UV irradiation or simvastatin immersion promoted osteogenic potential around the implants in the presence of bone graft material, even under conditions in which only a few cells and limited blood supply exist.

In both 2- and 4-week groups, in the native sides, there was no significant difference in the BA values between groups, whereas the BIC values differed significantly between group C and the experimental groups (group U, S, and SU). Moreover, in each group using a defined treatment option, there were statistically significant differences between the 2- and 4-week time points on the native sides: both BIC and BA in the control group; only BA in the experimental groups. Davies[61] described two different osteogenesis phenomena around dental implants: distance osteogenesis and contact osteogenesis. Distance osteogenesis occurs on the surface of an existing peri-implant bone through appositional growth, progressing toward the implant surface. Contact osteogenesis is de novo bone formation that occurs on the bioactive surface of the implant, and the orientation of bone growth is from implant to bone. On the native sides, distance osteogenesis from the nearby native bone would have greatly influenced new bone formation. Consequently,

it is presumed that there was no significant difference in the BA values between the experimental and the control groups on the native sides after 2 and 4 weeks postoperatively, respectively. The finding that the BIC values had already reached a plateau at 2 weeks in the experimental groups may be due to active contact osteogenesis resulting from the surface modification. The assumption that the effects of UV and simvastatin treatment of implants mainly occurred by the mechanism of contact osteogenesis seems logical enough since UV and simvastatin treatment was carried out on the surface of implants. Analysis on cellular level, such as counting the number of osteocytes initially attached to implant surface, would elucidate how active contact osteogenesis occurs on the surfaces treated with UV and simvastatin.

In this study, simvastatin was selected because of its widely proven osteogenic effect, both in cellular and animal studies. An in vitro study demonstrated that simvastatin increases mRNA expression levels of bone morphogenic protein-2 (BMP-2) in human MG-63 osteoblast-like cells.[29] Another study showed that simvastatin facilitates cell metabolism, proliferation and osteoblastic differentiation in human periodontal ligament cells.[62] At a small dose, simvastatin has been shown to improve periodontal hard tissue engineering by exerting an osteogenic potential in periodontal ligament stem cells.[63] In animal studies, local applications of simvastatin has been proven to reduce the amount of bone loss in an experimental periodontitis and aid in new bone formation of mandibular bone.[64,65]

However, statins have a low bone affinity, and much higher clinical doses than the lipid-lowering therapy are required to exert an influence on bone healing, resulting in

greater chances of systemic off-target effects of statins.[66] Through local delivery, the bioavailability of statins is increased, and the dose required for osseous healing is reduced. Consequently, the possibility of developing complications from systemic simvastatin use is lowered.[17,34] The local delivery method could increase the cost effectiveness by reducing the amount of simvastatin administered, further adding to its advantages. By immersing implants in simvastatin solution, clinicians can simply and safely apply a low concentration of simvastatin and acquire the desired outcomes in the peri-implant area.

In this study, implant surface was coated with simvastatin through a simple method of immersing implants into a simvastatin solution. Although local injection may be more reliable, repeated injections would be traumatic, hindering the healing process and carrying the risk of contamination. The author chose impregnation because it is simple, cost-effective, readily applicable, and does not require additional patient visits in clinical settings. The results indicated that simvastatin-coated implants improved osseointegration and new bone formation. However, simvastatin is only available for the first few hours through this method. To compensate for this limitation, the concentration of simvastatin was set to 0.5mM, which is higher than that used by other studies.[42,67-71] A slower, sustained release of the drug from implant surfaces may be favorable for osseointegration and bone healing. For example, the local application of simvastatin in poly-γ-glutamic acid gel has shown anabolic effects on the bone around titanium implants in rats.[72] Future studies should focus on optimizing the concentration and associated local delivery method of simvastatin

in clinical usage, which would form high-quality bone more rapidly and minimize the risk of undesired host/tissue reactions.

Higher BIC and BA values on the grafted sides were found in group S-4 compared to group C-4. This suggests that statins may be incorporated into bone augmentation techniques during implant surgery to achieve adequate bone quality and volume in a short time. To the author's knowledge, this was the first implant study to use simvastatin in conjunction with xenogeneic bone graft material. Implants coated with simvastatin add osteoinductivity to xenogeneic bone substitutes, which are known to possess osteoconductivity only. The combined effect of simvastatin and xenogeneic bone material resulted in superior osseointegration and osseous healing. This result is supported by a rabbit study by Wong and Rabie[21], who concluded that statin could be used alone in small defects or together with bone graft material to exert its osteoinductive effect in larger defects.

Moreover, the SLA surface-treated titanium implants were used in the present study, in line with similar studies that used simvastatin solution to facilitate osseointegration. In rat tibias, Yang et al.[73] placed implants that were roughened by large-grit blasting and acid etching; these were subsequently immersed in simvastatin solutions for drug adsorption onto implant surfaces. They observed that it improved osseointegration in the treated groups. Fang et al.[74] observed that large-grit blasted and acid-etched implants showed improved osseointegration in rat tibias when implant surfaces were coated with simvastatin. In agreement with those studies, the present study showed that simvastatin-

soaked SLA surface implants showed an improvement in osseous repair. Because the SLA surface has more wettability and surface energy than the machined surface, it may have facilitated adsorption of simvastatin molecules onto surfaces, consequently leading to better osseointegration.[75]

To date, several different mechanisms of UV photofunctionalization have been proposed. It was suggested that UV irradiation removes hydrocarbon contaminants from the titanium surface, which contributes to protein adsorption and cell attachment enabling more rapid osseointegration.[12,13] Additionally, UV-initiated photocatalytic activity alters the surface of grade IV titanium to produce lower reactive oxygen species levels than untreated titanium, providing a favorable environment for cellular adsorption and proliferation.[16] Moreover, it should be noted that UV irradiation is a well-known sterilization technique. The decreased likelihood of infection may have promoted the healing process. An in vitro study confirmed that UV treatment of titanium decreases the capability of human oral bacteria to form colonies in the presence of salivary and blood components.[76] The multi-beneficial actions of UV treatment would have contributed to osseointegration and bone healing in the UV-treated groups in this study.

Ueno et al.[15] described the use of UV-treated implants in a gap defect. They placed titanium rods that were treated with UV into a rat femur without being in contact with the innate cortical bone. They confirmed that the UV-treated implants in the gap healing condition resulted in bone–titanium integration with a strength equal to that of untreated implants in the contact healing condition. Accordingly, the present study indicated that UV

treatment of titanium increased the osteogenic potential effectively, even in an environment that lacks contact and support from the natural bone tissue. It could be stated that UV treatment was compatible with the xenogeneic bone graft material used in this study.

Simvastatin immersion followed by UV irradiation did not show a synergistic effect. Group SU did not yield better results than group U or S. Simvastatin is an organic compound composed of carbon skeletons, and it is probable that UV has broken down carbon skeletons by photon-induced radical reactions, the main mechanism by which UV cleanses titanium surface. When designing the experiment, the author speculated that the reverse sequence would result in diminished effect of UV due to the aging of titanium which occurs in a time-dependent fashion. Interestingly, a recent study by Choi et al.[16] revealed that immediate storage of UV-treated SLA implants in distilled water helps maintain photofunctionalized surface for up to 8 weeks. Future studies are recommended to discover if a synergistic effect of UV and simvastatin is observed when titanium is first treated with UV and then immediately stored in simvastatin solution. It should be noted that the concentration of simvastatin should be high enough to prevent other unwanted contaminants from adhering to titanium surface.

This study is liable to a few limitations. Due to the small number of samples per group and the usage of nonparametric statistical analyses, the statistical power may have been affected and therefore the results should be interpreted with caution. Although a single experienced operator placed implants under similar circumstances, the surgical technique could have influenced the outcomes. Each group of implants was placed in the

predetermined tibial location and side. This pre-allocated anatomical position may have influenced the result due to subtle differences in bone tissue and muscle movement. The differences among the groups regarding bone regeneration advancement may have been appreciated more thoroughly by applying staining techniques that distinguish newly formed bone, such as Masson's trichrome, Alizarin Red, or Von Kossa stains. Identifying bone-related molecular markers, including osteopontin and osteocalcin, would have provided further data on the extent of the osseointegration process. Moreover, the absence of occlusal forces, the histological differences between the rabbit tibia bone and human jawbones, and the low chance of infection may have introduced bias when interpreting the results.[40]

V. Conclusion

Within the limitations of this study, for a peri-implant bone defect in the rabbit tibia, histomorphometric analyses supported that UV irradiation or immersion of the implant in simvastatin solution has the potential to promote osseointegration and new bone formation around titanium implants, with or without xenogeneic bone graft material. However, no synergistic effect of the two treatments was observed. Based on the findings of this study, UV irradiation or simvastatin immersion could be helpful in promoting osseointegration and osseous healing when placing implants in freshly extracted sockets with osteoconductive grafts. Both treatments would function as supplements to clinicians encountering the challenges of immediate implantation and may lead to novel strategies for early implant restorations.

REFERENCES

1. Şimşek S, Özeç İ, Kürkçü M, Benlidayı E. Histomorphometric evaluation of bone formation in peri-implant defects treated with different regeneration techniques: An experimental study in a rabbit model. J Oral Maxillofac Surg 2016;74(9):1757–64.
2. Ebenezer V, Balakrishnan K, Asir RVD, Sragunar B. Immediate placement of endosseous implants into the extraction sockets. J Pharm Bioallied Sci 2015;7(Suppl 1):S234–7.
3. Becker W. Immediate implant placement: Treatment planning and surgical steps for successful outcomes. Br Dent J 2006;201(4):199–205.
4. Kahnberg K-E. Immediate implant placement in fresh extraction sockets: A clinical report. Int J Oral Maxillofac Implant 2009;24(2):282–8.
5. Zitzmann NU, Naef R, Schärer P. Resorbable versus nonresorbable membranes in combination with Bio-oss for guided bone regeneration. Int J Oral Maxillofac Implant 1997;12(6):220–38.
6. Lorenzoni M, Pertl C, Keil C, Wegscheider WA. Treatment of peri-implant defects with guided bone regeneration: A comparative clinical study with various membranes and bone grafts. Int J Oral Maxillofac Implant 1998;13(5):639–46.
7. Van Steenberghe D, Callens A, Geers L, Jacobs R. The clinical use of deproteinized bovine bone mineral on bone regeneration in conjunction with immediate implant installation. Clin Oral Implant Res 2000;11(3):210–6.

8. Ortega-Martínez J, Pérez-Pascual T, Mareque-Bueno S, Hernández-Alfaro F, Ferrés-Padró E. Immediate implants following tooth extraction. A systematic review. Med Oral Patol Oral Cir Bucal 2012;17(2):e251.
9. Brånemark P-I. Osseointegrated implants in the treatment of the edentulous jaw. Experience from a 10-year period. Scand J Plast Reconstr Surg Suppl 1977;16:1–132.
10. Carlsson L, Rostlund T, Albrektsson B, Albrektsson T, Brånemark P-I. Osseointegration of titanium implants. Acta Orthop Scand 1986;57(4):285–9.
11. Chang PC, Lang NP, Giannobile WV. Evaluation of functional dynamics during osseointegration and regeneration associated with oral implants. Clin Oral Implant Res 2010; 21(1):1–12.
12. Aita H, Hori N, Takeuchi M, Suzuki T, Yamada M, Anpo M, Ogawa T. The effect of ultraviolet functionalization of titanium on integration with bone. Biomaterials 2009;30(6):1015–25.
13. Att W, Hori N, Iwasa F, Yamada M, Ueno T, Ogawa T. The effect of UV-photofunctionalization on the time-related bioactivity of titanium and chromium-cobalt alloys. Biomaterials 2009;30(26):4268–76.
14. Jeon C, Oh KC, Park K-H, Moon HS. Effects of ultraviolet treatment and alendronate immersion on osteoblast-like cells and human gingival fibroblasts cultured on titanium surfaces. Sci Rep 2019;9(1):1–11.

15. Ueno T, Yamada M, Suzuki T, Minamikawa H, Sato N, Hori N, et al. Enhancement of bone–titanium integration profile with UV-photofunctionalized titanium in a gap healing model. Biomaterials 2010;31(7):1546–57.
16. Choi S-H, Ryu J-H, Kwon J-S, Kim J-E, Cha J-Y, Lee K-J, et al. Effect of wet storage on the bioactivity of ultraviolet light-and non-thermal atmospheric pressure plasma-treated titanium and zirconia implant surfaces. Materials Science and Engineering: C 2019;105:110049.
17. Kim HS, Lee JI, Yang SS, Kim BS, Kim BC, Lee J. The effect of alendronate soaking and ultraviolet treatment on bone–implant interface. Clin Oral Implant Res 2017;28(9):1164–72.
18. Lee J-B, Jo Y-H, Choi J-Y, Seol Y-J, Lee Y-M, Ku Y, Rhyu I-C, Yeo I-SL. The effect of ultraviolet photofunctionalization on a titanium dental implant with machined surface: An in vitro and in vivo study. Materials 2019;12(13):2078.
19. Park K-H, Koak J-Y, Kim S-K, Han C-H, Heo S-J. The effect of ultraviolet-c irradiation via a bactericidal ultraviolet sterilizer on an anodized titanium implant: A study in rabbits. Int J Oral Maxillofac Implant 2013;28(1):57–66.
20. Roy M, Pompella A, Kubacki J, Szade J, Roy RA, Hedzelek W. Photofunctionalization of titanium: An alternative explanation of its chemical-physical mechanism. PLoS ONE 2016;11(6):e0157481.
21. Wong RWK, Rabie ABM. Statin collagen grafts used to repair defects in the parietal bone of rabbits. Br J Oral Maxillofac Surg 2003;41(4):244–8.

22. Serro A, Saramago B. Influence of sterilization on the mineralization of titanium implants induced by incubation in various biological model fluids. Biomaterials 2003;24(26):4749–60.
23. Zhang H, Komasa S, Mashimo C, Sekino T, Okazaki J. Effect of ultraviolet treatment on bacterial attachment and osteogenic activity to alkali-treated titanium with nanonetwork structures. Int J Nanomed 2017;12:4633–46.
24. Kellesarian SV, Al Amri MD, Al-Kheraif AA, Ghanem A, Malmstrom H, Javed F. Efficacy of local and systemic statin delivery on the osseointegration of implants: A systematic review. Int J Oral Maxillofac Implant 2017;32(3):497–506.
25. Chuengsamarn S, Rattanamongkoulgul S, Suwanwalaikorn S, Wattanasirichaigoon S, Kaufman L. Effects of statins vs. non-statin lipid-lowering therapy on bone formation and bone mineral density biomarkers in patients with hyperlipidemia. Bone 2010;46(4):1011–5.
26. Skoglund B, Forslund C, Aspenberg P. Simvastatin improves fracture healing in mice. J Bone Miner Res 2002;17(11):2004–8.
27. Ruan F, Zheng Q, Wang J. Mechanisms of bone anabolism regulated by statins. Biosci Rep 2012;32(6):511–9.
28. Chen P-Y, Sun J-S, Tsuang Y-H, Chen M-H, Weng P-W, Lin F-H. Simvastatin promotes osteoblast viability and differentiation via Ras/Smad/Erk/BMP-2 signaling pathway. Nutr Res 2010;30(3):191–9.

29. Mundy G, Garrett R, Harris S, Chan J, Chen D, Rossini G, et al. Stimulation of bone formation in vitro and in rodents by statins. Science 1999;286(5446):1946–9.
30. Song C, Guo Z, Ma Q, Chen Z, Liu Z, Jia H. Simvastatin induces osteoblastic differentiation and inhibits adipocytic differentiation in mouse bone marrow stromal cells. Biochem Biophys Res Commun 2003;308(3):458–62.
31. Li X, Song Q-S, Wang J-Y, Leng H-J, Chen Z-Q, Liu Z-J, Dang G-T, Song C-L. Simvastatin induces estrogen receptor-alpha expression in bone, restores bone loss, and decreases ERα expression and uterine wet weight in ovariectomized rats. J Bone Miner Metab 2011;29(4):396–403.
32. Hwang R, Lee EJ, Kim MH, Li S-Z, Jin Y-J, Rhee Y, et al. Calcyclin, a Ca2+ ion-binding protein, contributes to the anabolic effects of simvastatin on bone. J Biol Chem 2004;279(20):21239–47.
33. Laufs U, La Fata V, Liao JK. Inhibition of 3-hydroxy-3-methylglutaryl (HMG)-CoA reductase blocks hypoxia-mediated down-regulation of endothelial nitric oxide synthase. J Biol Chem 1997;272(50):31725–9.
34. Oryan A, Kamali A, Moshiri A. Potential mechanisms and applications of statins on osteogenesis: Current modalities, conflicts and future directions. J Control Release 2015;215:12–24.
35. Yamashita M, Otsuka F, Mukai T, Yamanaka R, Otani H, Matsumoto Y, et al. Simvastatin inhibits osteoclast differentiation induced by bone morphogenetic

protein-2 and RANKL through regulating MAPK, AKT and Src signaling. Regul Pept 2010;162(1-3):99–108.

36. Apostu D, Lucaciu O, Mester A, Oltean-Dan D, Gheban D, Rares Ciprian Benea H. Tibolone, alendronate, and simvastatin enhance implant osseointegration in a preclinical in vivo model. Clin Oral Implant Res 2020;31(7):655–68.
37. Fu JH, Bashutski JD, Al-Hezaimi K, Wang HL. Statins, glucocorticoids, and nonsteroidal anti-inflammatory drugs: Their influence on implant healing. Implant Dent 2012;21(5):362–7.
38. Tan J, Yang N, Fu X, Cui Y, Guo Q, Ma T. Single-dose local simvastatin injection improves implant fixation via increased angiogenesis and bone formation in an ovariectomized rat model. Med Sci Monit 2015;21:1428–39.
39. Gupta S, Del Fabbro M, Chang J. The impact of simvastatin intervention on the healing of bone, soft tissue, and TMJ cartilage in dentistry: A systematic review and meta-analysis. Int J Implant Dent 2019;5(1):17.
40. Moraschini V, Almeida DCF, Calasans-Maia JA, Diuana Calasans-Maia M. The ability of topical and systemic statins to increase osteogenesis around dental implants: A systematic review of histomorphometric outcomes in animal studies. Int J Oral Maxillofac Surg 2018;47(8):1070-8.
41. Dos Santos PL, de Molon RS, Queiroz TP, Okamoto R, de Souza Faloni AP, Gulinelli JL et al. Evaluation of bone substitutes for treatment of peri-implant bone

defects: Biomechanical, histological, and immunohistochemical analyses in the rabbit tibia. J Periodontal Implant Sci 2016;46(3):176–96.

42. Faraco-Schwed FN, Mangueira LM, Ribeiro JV, Antao Ada S, Shibli JA. Removal torque analysis of implants in rabbit tibia after topical application of simvastatin gel. J Oral Implantol 2014;40(1):53–9.
43. Mapara M, Thomas BS, Bhat K. Rabbit as an animal model for experimental research. Dent Res J 2012;9(1):111–8.
44. Ribeiro M, Fraguas EH, Brito KIC, Kim YJ, Pallos D, Sendyk WR. Bone autografts & allografts placed simultaneously with dental implants in rabbits. J Craniomaxillofac Surg 2018;46(1):142–7.
45. Stübinger S, Dard M. The rabbit as experimental model for research in implant dentistry and related tissue regeneration. J Investig Surg 2013;26(5):266–82.
46. Kim Y-K, An Y-Z, Cha J-K, Lee J-S, Jung U-W, Choi S-H. Combined effects of a chemically cross-linked porcine collagen membrane and highly soluble biphasic calcium phosphate on localized bone regeneration. J Korean Dent Assoc 2018;56:667–85.
47. Flanagan D. Photofunctionalization of dental implants. J Oral Implantol 2016;42(5):445–50.
48. Henningsen A, Smeets R, Hartjen P, Heinrich O, Heuberger R, Heiland M. Photofunctionalization and non-thermal plasma activation of titanium surfaces. Clin Oral Investig 2018;22(2):1045–54.

49. Arifin WN, Zahiruddin WM. Sample size calculation in animal studies using resource equation approach. Malays J Med Sci 2017;24(5):101.
50. Ilyas M, Adzim M, Simbak N, Atif A. Sample size calculation for animal studies using degree of freedom (E); an easy and statistically defined approach for metabolomics and genetic research. ILAR J 2017;43(4):207–13.
51. Donath K, Breuner G. A method for the study of undecalcified bones and teeth with attached soft tissues. The Säge-Schliff (sawing and grinding) technique. J Oral Pathol Med 1982;11(4): 318–26.
52. Duncan WJ, Gay JH, Lee MH, Bae TS, Lee SJ, Loch C. The effect of hydrothermal spark discharge anodization in the early integration of implants in sheep sinuses. Clin Oral Implant Res 2016;27(8):975–80.
53. Duncan WJ, Lee MH, Bae TS, Lee SJ, Gay J, Loch C. Anodisation increases integration of unloaded titanium implants in sheep mandible. Biomed Res Int 2015;2015:857969.
54. Yoo SY, Kim SK, Heo SJ, Koak JY, Lee JH, Heo JM. Biochemical responses of anodized titanium implants with a poly(lactide-co-glycolide)/bone morphogenetic protein-2 submicron particle coating. Part 2: An in vivo study. Int J Oral Maxillofac Implant 2015;30(4):754–60.
55. Littuma GJS, Sordi MB, Borges Curtarelli R, Aragones A, da Cruz ACC, Magini RS. Titanium coated with poly(lactic-co-glycolic) acid incorporating simvastatin:

Biofunctionalization of dental prosthetic abutments. J Periodontal Res 2020;55(1):116–24.

56. SreeHarsha N, Hiremath JG, Sarudkar S, Attimarad M, Al-Dhubiab B, Balachandran Nair A, Venugopala KN, Asif AH. Spray dried amorphous form of simvastatin: Preparation and evaluation of the buccal tablet. Indian J Pharm Educ Res 2019;54(1):46–54.
57. Sawase T, Jimbo R, Baba K, Shibata Y, Ikeda T, Atsuta M. Photo-induced hydrophilicity enhances initial cell behavior and early bone apposition. Clin Oral Implant Res 2008;19(5):491-6.
58. Albrektsson T, Brånemark PI, Hansson HA, Lindstrom J. Osseointegrated titanium implants. Requirements for ensuring a long-lasting, direct bone-to-implant anchorage in man. Acta Orthop Scand 1981;52(2):155–70.
59. Gallucci GO, Hamilton A, Zhou W, Buser D, Chen S. Implant placement and loading protocols in partially edentulous patients: A systematic review. Clin Oral Implant Res 2018;29(Suppl. 16):106–34.
60. Araújo M, Linder E, Lindhe J. Effect of a xenograft on early bone formation in extraction sockets: An experimental study in dog. Clin Oral Implant Res 2009;20(1):1–6.
61. Davies J. Mechanisms of endosseous integration. Int J Prosthodont 1998;11(5):391–401.

62. Yazawa H, Zimmermann B, Asami Y, Bernimoulin J-P. Simvastatin promotes cell metabolism, proliferation, and osteoblastic differentiation in human periodontal ligament cells. J Periodontol 2005;76(2):295-302
63. Zhao BJ, Liu YH. Simvastatin induces the osteogenic differentiation of human periodontal ligament stem cells. Fundam Clin Pharmacol 2014;28(5):583-92.
64. Özeç I, Kiliç E, Gümüs C, Göze F. Effect of local simvastatin application on mandibular defects. 2007;18(3):546-50.
65. Stein D, Lee Y, Schmid MJ, Killpack B, Genrich MA, Narayana N, et al. Local simvastatin effects on mandibular bone growth and inflammation. 2005;76(11):1861-70.
66. Oryan A, Alidadi S, Moshiri A, Maffulli N. Bone regenerative medicine: classic options, novel strategies, and future directions. J Orthop Surg Res 2014;9(1):1-27.
67. Zhang S, Matsushita T, Kuroda R, Nishida K, Matsuzaki T, Matsumoto T, et al. Local administration of simvastatin stimulates healing of an avascular meniscus in a rabbit model of a meniscal defect. Am J Sports Med 2016;44:1735–43.
68. Zhao B, Li X, Xu H, Jiang Y, Wang D, Liu R. Influence of simvastatin-strontium-hydroxyapatite coated implant formed by micro-arc oxidation and immersion method on osteointegration in osteoporotic rabbits. Int J Nanomedicine 2020;15:1797-807.

69. Zhao S, Wen F, He F, Liu L, Yang G. In vitro and in vivo evaluation of the osteogenic ability of implant surfaces with a local delivery of simvastatin. Int J Oral Maxillofac Implant 2014;29(1):211–20.

70. Başarır K, Erdemli B, Can A, Erdemli E, Zeyrek T. Osseointegration in arthroplasty: Can simvastatin promote bone response to implants? Int Orthop 2009;33(3):855–9.

71. Lian-yi X, Xiao-juan S, Xiu-li Z, Yu-qin J, Yu-qiong W, Xin-quan J. Repair of calvarial defect using a tissue-engineered bone with simvastatin-loaded β-tricalcium phosphate scaffold and adipose derived stem cells in rabbits. Shanghai J Stomatol 2013;22(4):361–7.

72. Moriyama Y, Ayukawa Y, Ogino Y, Atsuta I, Todo M, Takao Y, et al. Local application of fluvastatin improves peri-implant bone quantity and mechanical properties: A rodent study. Acta Biomater 2010;6(4):1610–8.

73. Yang G, Song L, Guo C, Zhao S, Liu L, He F. Bone responses to simvastatin-loaded porous implant surfaces in an ovariectomized model. Int J Oral Maxillofac Implant 2012;27(2):369–74.

74. Fang W, Zhao S, He F, Liu L, Yang G. Influence of simvastatin-loaded implants on osseointegration in an ovariectomized animal model. BioMed Res Int 2015;2015:831504.

75. Feller L, Jadwat Y, Khammissa RA, Meyerov R, Schechter I, Lemmer J. Cellular responses evoked by different surface characteristics of intraosseous titanium implants. BioMed Res Int 2015;2015:171945.

76. de Avila ED, Lima BP, Sekiya T, Torii Y, Ogawa T, Shi W. Effect of UV-photofunctionalization on oral bacterial attachment and biofilm formation to titanium implant material. Biomaterials 2015;67:84–92.

ABSTRACT (Korean)

자외선 조사 및 심바스타틴 침지를 이용한 표면처리가 토끼의 경골에 식립한 티타늄 임플란트에 미치는 영향

전 지 훈

연세대학교 대학원 치의학과 (지도교수 문 홍 석)

본 연구에서는 토끼의 경골에 큰 입자를 표면에 분사하고 산부식한 표면을 가진 SLA (sandblasted, large-grit, acid-etched) 티타늄 치과 임플란트에 자외선 조사 및 심바스타틴 침지를 하였을 때 골유착에 어떠한 영향을 미치는지 두 가지 시점(時点)에서 평가하였다. 임플란트는 표면처리 방법에 따라 네 가지 군으로 분류되었다. 열 두 마리의 토끼에 대하여 한 경골 당 두 개의 임플란트를 식립하였다. 트레핀 버를 이용해 경골에 원형 결손부를 형성하였고, 임플란트가 골 표면에 접촉할 수 있도록 결손부의 한 쪽에 기대어 식립하였으며 간격에는 소 뼈 이식재를 채워 넣었다. 토끼는 2주 또는 4주 후 희생되었다. 자외선 조사 또는 심바스타틴 침지는 골 이식을 하지 않은 부위에서 골-임플란트 접촉(bone-to-implant contact,

BIC)을 유의하게 증가시켰고, 골 이식을 한 부위에서는 BIC 와 골 면적(bone area, BA)를 모두 유의하게 증가시켰다. 두 방법을 모두 적용하는 것은 단일 방법을 적용하는 것과 비교하였을 때 더 나은 결과를 보이지 않았다. 이상의 결과에 따라, SLA 티타늄 임플란트에 자외선 조사 또는 심바스타틴 침지를 하는 것은 토끼의 경골에서 골유착과 신생골 형성을 촉진한다고 결론지을 수 있다.

핵심 되는 말: 동물 실험, 골 임플란트 상호작용, 골 이식재, 골 재생, 심바스타틴, 자외선, 티타늄